AGU100 ADVANCING EARTH AND SPACE SCIENCE

Geophysical Research Letters

RESEARCH LETTER
10.1029/2018GL079455

Key Points:
- Centennial-scale variability in the tropical Pacific emerges in some climate models from ocean's integration of higher-frequency noise
- Models with El Niño-Southern Oscillation variance that is too large in the western Pacific exhibit stronger centennial-scale variability
- Multimodel ensemble interpretations require a cautious evaluation because of biases in centennial variability in the tropical Pacific

Supporting Information:
- Supporting Information S1

Correspondence to:
D. Samanta,
dhruba@ntu.edu.sg

Citation:
Samanta, D., Karnauskas, K. B., Goodkin, N. F., Coats, S., Smerdon, J. E., & Zhang, L. (2018). Coupled model biases breed spurious low-frequency variability in the tropical Pacific Ocean. *Geophysical Research Letters*, *45*, 10,609–10,618. https://doi.org/10.1029/2018GL079455

Received 3 JUL 2018
Accepted 13 SEP 2018
Accepted article online 17 SEP 2018
Published online 7 OCT 2018

Coupled Model Biases Breed Spurious Low-Frequency Variability in the Tropical Pacific Ocean

Dhrubajyoti Samanta[1], Kristopher B. Karnauskas[2,3], Nathalie F. Goodkin[1,4,5], Sloan Coats[6], Jason E. Smerdon[7], and Lei Zhang[3]

[1]Asian School of the Environment, Nanyang Technological University, Singapore, [2]Cooperative Institute for Research in Environmental Science, University of Colorado Boulder, Boulder, CO, USA, [3]Department of Atmospheric and Oceanic Sciences, University of Colorado Boulder, Boulder, CO, USA, [4]Earth Observatory of Singapore, Singapore, [5]Department of Earth and Planetary Sciences, American Museum of Natural History, New York, NY, USA, [6]Department of Geology and Geophysics, Woods Hole Oceanographic Institution, Woods Hole, MA, USA, [7]Lamont-Doherty Earth Observatory, Columbia University, New York, NY, USA

Abstract Coupled general circulation model (GCM) biases in the tropical Pacific are substantial, including a westward extended cold sea surface temperature (SST) bias linked to El Niño–Southern Oscillation (ENSO). Investigation of internal climate variability at centennial timescales using multicentury control integrations of 27 GCMs suggests that a Pacific Centennial Oscillation emerges in GCMs with too strong ENSO variability in the equatorial Pacific, including westward extended SST variability. Using a stochastic model of climate variability (Hasselmann type), we diagnose such centennial SST variance in the western equatorial Pacific. The consistency of a simple stochastic model with complex GCMs suggests that a previously defined Pacific Centennial Oscillation may be driven by biases in high-frequency ENSO forcing in the western equatorial Pacific. A cautious evaluation of long-term trends in the tropical Pacific from GCMs is necessary because significant trends in historical and future simulations are possible consequences of biases in simulated internal variability alone.

Plain Language Summary The tropical Pacific Ocean exhibits natural climate variability on a wide range of timescales, some of which are similar to the length of instrumental records (~100 years). Characterizing natural cycles with periods of ~100 years is therefore important for detecting and attributing human forced changes. Analysis of climate model simulations shows that a previously defined 100-year cycle in tropical Pacific sea surface temperatures is the result of mismatches between the models and the real world and therefore may not exist in reality. Our results show that a 100-year periodicity in the tropical Pacific Ocean is a robust feature of models with an erroneously strong El Niño pattern in the western Pacific Ocean including wind fluctuations. We reveal the causes of 100-year cycles in the western Pacific, which relies on the ocean's large thermal capacity to smooth out frequent short-term wind events into slower cycles. Our study highlights the need for cautious interpretations of trends in the tropical Pacific Ocean from climate models due to these possibly spurious 100-year cycles, especially for attributing historical changes and predicting future climate. If these model mismatches can be corrected, it may allow more accurate predictions of El Niño and long-term trends over 21st century.

1. Introduction

The dominant influence of the tropical Pacific on global interannual to centennial climate variability has motivated considerable interest in exploring its response to anthropogenic forcing (Cai et al., 2015; Hua et al., 2018; Karnauskas et al., 2012). On longer timescales, the variability of the tropical Pacific is less well characterized due to the paucity of long observational records (e.g., Deser et al., 2004). As a result, long control simulations from fully coupled general circulation models (GCMs) with constant external forcing remains a primary means to study the low-frequency internal variability of the tropical Pacific for climate change detection, attribution, and model evaluation (e.g., Collins et al., 2001). Using the available long control runs from three Coupled Model Intercomparison Project Phase 3 (CMIP3) generation GCMs, Karnauskas et al. (2012) characterized a potential mode of internal climate variability over the tropical Pacific, named the Pacific Centennial Oscillation (PCO), with impacts on the equatorial Pacific zonal sea surface temperature (SST) gradient (west-minus-east) of roughly a half a degree centigrade. Such a change is equivalent to estimated

trends over the observational interval since approximately 1900 (Coats & Karnauskas, 2017). Karnauskas et al. (2012) hypothesized a few possible implications of the PCO in GCMs, such as the impact of a possible counterpart in nature, and also the possibility that the PCO in GCMs may be a spurious artifact of coupled models. If the PCO is also present in newer-generation GCMs, then future trends projected by these GCMs may be strongly controlled by the interplay between external forcing and internal variability at centennial timescales. Regardless of whether the PCO has a counterpart in nature, it is thus important to consider the possible presence of the PCO when attempting to isolate forced changes from simulated internal variability in coupled model simulations. This endeavor is critical because the nature of future changes in the tropical Pacific, especially changes in SST and SST-driven atmospheric circulation anomalies, will impact the response of the broader climate system to global warming, with subtle but important implications for regional hydroclimate (Karnauskas et al., 2009; Seager et al., 2009; Seager & Vecchi, 2010).

Paleoclimate archives indicate that low-frequency variability in the tropical Pacific may be more prominent than implied by instrumental records (Cobb et al., 2003; Tierney et al., 2010). However, it is not well understood how external forcing and internal dynamics generate variability at timescales greater than decadal (Ault et al., 2013, 2018; Coats & Karnauskas, 2017; Coats et al., 2016). Earlier studies suggest decadal-to-centennial variability may develop in GCMs as a residual of energetic interannual variability (Newman et al., 2011; Wittenberg, 2009), resulting from slowly varying ocean-atmosphere interactions not associated with the El Niño–Southern Oscillation (ENSO; Clement & Cane, 1999; Zebiak & Cane, 1991) or from deterministic processes (Meehl & Hu, 2006; Wittenberg, 2009). Low-frequency variability in the tropical Pacific even arises from unforced atmospheric general circulation models coupled to a simple slab ocean (Clement et al., 2011; Dommenget & Latif, 2008).

Tropical Pacific climate variability on interannual timescales is dominated by ENSO (Philander, 2001; Trenberth & Hurrell, 1994), which has broad societal implications (McPhaden et al., 2006). However, one of the largest existing uncertainties in our understanding of the tropical Pacific is the relationship between its mean-state and ENSO (Cobb et al., 2003; Kim et al., 2014; McPhaden et al., 2011; Philander & Fedorov, 2003), in terms of ENSO dynamics, impacts, and predictability. Despite improvements in the simulations of ENSO by GCMs, recent multimodel analyses indicate serious systematic biases in the simulated mean climate (Capotondi et al., 2006; Guilyardi, 2005; van Oldenborgh et al., 2005), such as errors in simulating the equatorial Pacific cold tongue and intertropical convergence zone (Li & Xie, 2014). The complex interactions between these mean-state biases and ENSO, together with GCM structural diversity, make it difficult to unambiguously diagnose deficiencies in simulating ENSO (Guilyardi et al., 2009). For instance, the state of the eastern equatorial Pacific Ocean is closely related to ENSO; however, GCMs produce a cold tongue with a cold bias, including a westward extension (e.g., Harrison et al., 2002; Karnauskas et al., 2007). This imposes a major obstacle to the realistic simulation of tropical clouds, precipitation, and ocean-atmospheric coupling that are crucial for representing ENSO dynamics.

In this study, we aim to evaluate whether the PCO remains a characteristic feature in all of the most recent generation of GCMs. We also explore mechanisms that generate low-frequency variability in the tropical Pacific including those that may be related to systematic biases in coupled models that affect both the mean-state and interannual variability. Despite common biases, many GCMs do show a diversity in ENSO behavior in terms of amplitude, period, and spatial extension (Capotondi et al., 2015; Guilyardi et al., 2009; Lemmon & Karnauskas, 2018), but an examination of the impact of such diversity on low-frequency variability is not considered in the present study.

2. Models and Methods

We use preindustrial control runs from 26 CMIP5 models (Taylor et al., 2012) and the Community Earth System Model (CESM) Large Ensemble Project (LENS) (Kay et al., 2015). These 27 GCMs were selected based on the availability of control simulations spanning at least 500 years (Table S1 in the supporting information), as our focus here is to detect and understand centennial-scale variability. We analyzed three output variables from these model simulations: SST, surface zonal wind speed (u10), and ocean mixed layer depth (MLD). For the CMIP5 models, we used surface skin temperature from the atmospheric component throughout; however, we refer to this as SST for brevity and because the surface temperature is nearly equivalent to SST, especially at longer timescales when surface fluxes lead to sufficient equilibrium along the atmosphere and ocean

interface. Annually resolved data for all variables were analyzed over the tropical Pacific, and these were transformed into a common grid of 2.0° × 1.5° (however, 2.0° × 2.0° for MLD) using bilinear interpolation before calculating any multimodel composite.

A leading empirical orthogonal function analysis of centennial-scale SST was used to identify the dominant structures of centennial-scale variability in the tropical Pacific (see Figure 5 in Karnauskas et al., 2012). We find that not all 27 GCMs exhibit a leading zonal dipole mode in centennial SST variability (Figure S1) that is characteristic of the PCO as defined by Karnauskas et al. (2012). Moreover, these GCMs show a diversity in the longitudinal extent of SST variability in the equatorial Pacific (Figures S2–S3), which is closely related to ENSO variability. Given the range of characteristics, we categorized the models into two groups (a. Type 1 ENSO models and b. Type 2 ENSO models) based on the magnitude of boreal wintertime (December–February, DJF) mean-state SST variability over the western equatorial Pacific compared to 2 times DJF SST values from observations, obtained from COBE SST version 2 (https://www.esrl.noaa.gov/psd/data/gridded/data.cobe2.html; Figure 1a). This longitudinal reference point for categorization of the models is selected based on a clear separation point among the SST variability profiles (Figure 1a) over the western equatorial Pacific. However, empirical testing indicates that our main conclusions are not sensitive to the selected longitudinal location (see Figure S4). More broadly, this choice was made to assess the impact of differences in the tropical Pacific mean-state and interannual variability on the simulation of centennial-scale variability, without making prior assumptions about the spatial pattern and characteristics of such variability. Models with higher SST variability on the equator than 2 times observed (0.88 °C) at 164°E are characterized as Type 1 ENSO models and the rest as Type 2 ENSO models (Figure 1a). The list of GCMs from these two groups with model details are provided in Table S1; 9 and 18 models are found to be Type 1 and Type 2 ENSO models, respectively. Compared to observations (Figure 1b), the composite spatial patterns of SST variability for Type 1 ENSO models clearly indicate higher SST variability throughout the equatorial Pacific, including westward extension (Figure 1c). Type 2 ENSO models (Figure 1d) exhibit a longitudinal extension of SST variability more similar to observations, implying more realistic ENSO variability in these models. The extension of high-frequency SST variability up to the maritime continent in Type 1 ENSO models is suggestive of an injection of high-frequency, largely stochastic variability in the Indo-Pacific warm pool region, which likely has further consequences for climate variability over the tropical Pacific.

The simplest paradigm for characterizing climate variability defines the coupled ocean-atmosphere system as a first-order Markov process (red noise) in which internal climate variability increases in magnitude at longer timescales due to the thermal inertia of the ocean and the associated *reddening* of a stochastic input (Hasselmann, 1976). We use this approach (Hasselmann, 1976) to explore the generation of low-frequency SST variability and the possible predictability of the PCO in the real ocean. The Hasselmann (1976) model for a slab mixed layer model forced by atmospheric noise, is defined by the following equation

$$\rho c H \frac{dT}{dt} = A - \lambda T \tag{1}$$

where ρ, c, H, T, A, and λ denote the density of seawater, heat capacity of seawater, MLD, SST, white atmospheric noise, and fixed thermal damping parameter, respectively.

This simple model is a well-known paradigm for understanding ocean-atmosphere interactions by demonstrating how low-frequency variability can arise because of the ocean integrating high-frequency, stochastic atmospheric variability. In the specific case considered herein, annual equatorial wind stress variability serves as the source of the high-frequency noise. In the original work of Hasselmann (1976), surface heat flux was used as the high-frequency noise A. The choice of surface variable is not critical, however, because as for the purposes herein the variable is used only to define inter-model differences in the *amplitude* of the noise forcing (Figure S5).

3. Results

To characterize the annual mean-state in the Type 1 and Type 2 ENSO models, we analyzed the composite difference of mean SST fields in these model simulations. The climatology of the tropical Pacific is characterized by strong zonal asymmetry, with an eastern equatorial cold tongue. Ocean-atmosphere interactions play

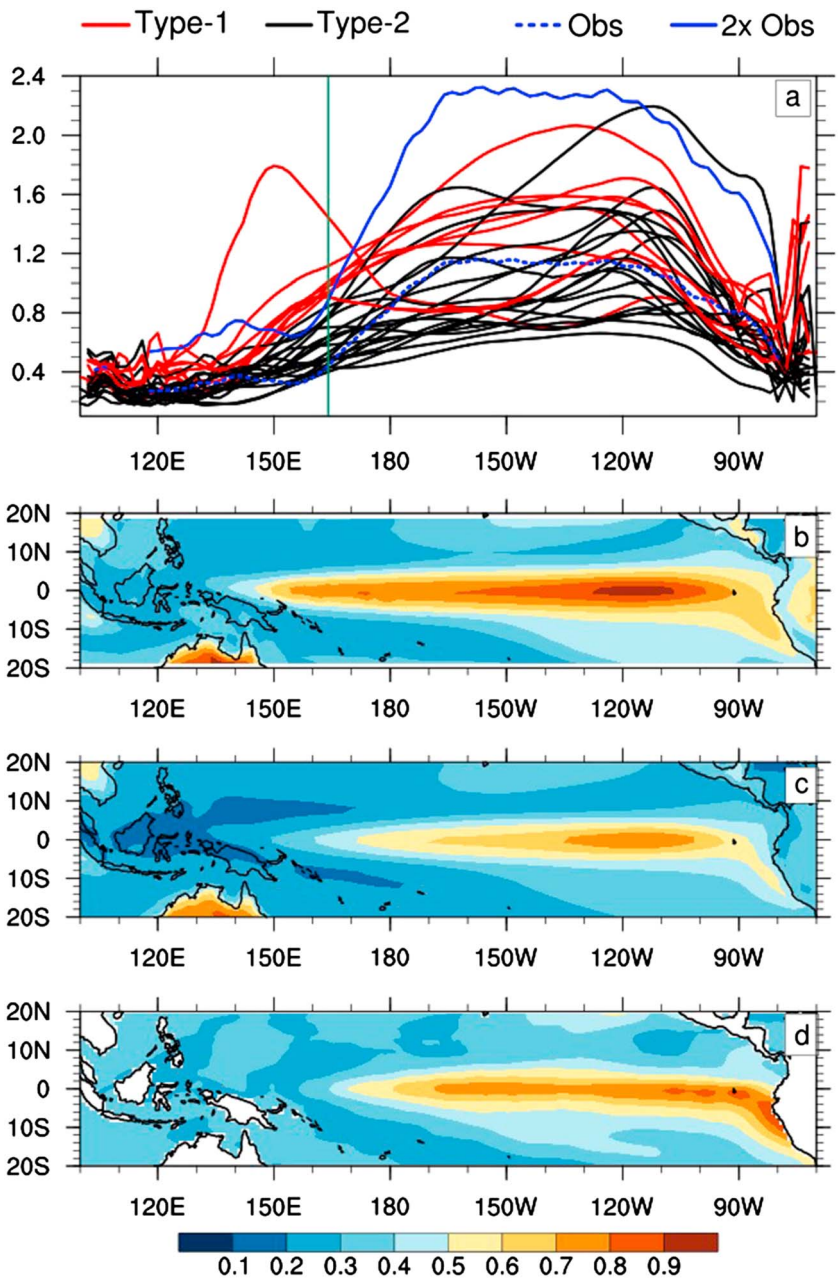

Figure 1. Categorization of models based on boreal wintertime equatorial SST variability and spatial pattern of annual SST variability (°C). (a) The standard deviation of equatorial (averaged over 2.5°S to 2.5°N) unfiltered December-January-February SST for Type 1 ENSO models (red), Type 2 ENSO models (black), observed SST (dashed blue line), and two times observed December-January-February SST (solid blue line). The models are categorized into two groups with respect to the equatorial reference point of 0.88 °C and 164°E (green vertical line = reference longitude); the standard deviation of unfiltered annual SST for (b) composite Type 1, (c) composite Type 2 ENSO models, and (d) observations. SST = sea surface temperature; ENSO = El Niño–Southern Oscillation.

a critical role in generating and maintaining this asymmetric feature despite zonally uniform and symmetric solar radiation at the top of the atmosphere (Xie et al., 2007). Along the equator, the interaction of easterly winds and the cold tongue is key for maintaining the zonal asymmetry (Sun & Liu, 1996). However, the Type 1 ENSO models clearly indicate a cold tongue SST bias extending to the maritime continent unlike Type 2 ENSO models (Figure 2a). The westward extent of this bias is colocated with a region of abnormally high SST variability (Figure 1c) in these models, likely related to biases in ENSO variability. Therefore, in

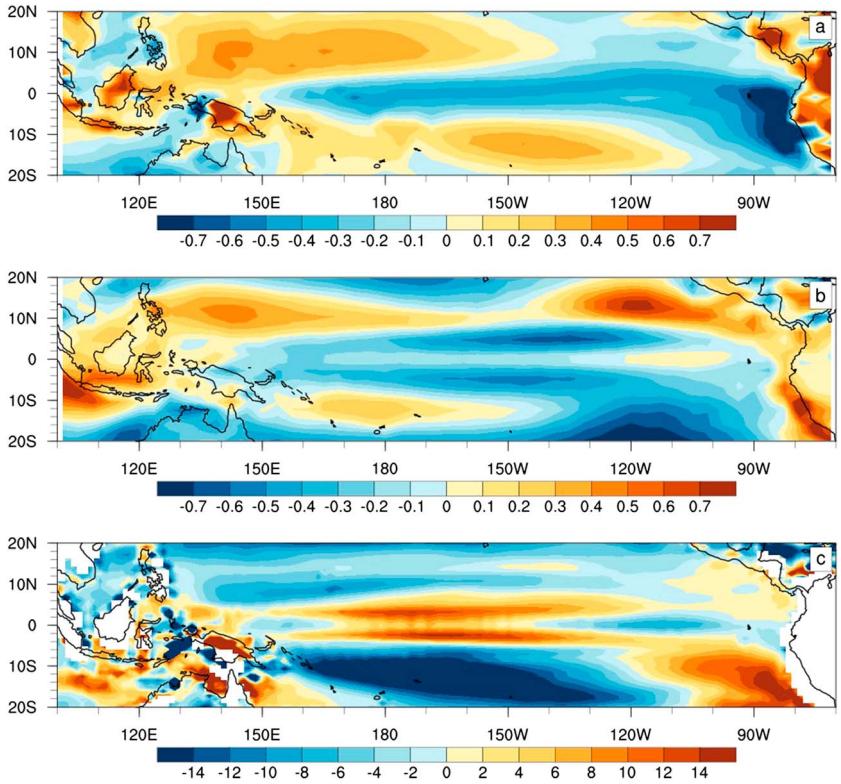

Figure 2. Composite annual mean-state difference between two types of models (Type 1 and Type 2 El Niño–Southern Oscillation models). Unfiltered annual fields for (a) sea surface temperature (°C), (b) surface zonal wind speed (m/s), and (c) mixed layer depth (m).

Type 1 ENSO models there appears to be a close relationship between the mean bias in SST and ENSO, and biases in u10 (Figure 2b). Specifically, analysis of u10 (Figure 2b) indicates stronger easterlies and thereby intense westward surface currents in the eastern Pacific in Type 1 ENSO models, implying a potential role for the westward advection of cold surface water from the east to the maritime continent. Due to stronger u10, MLD also becomes deeper in the central equatorial Pacific in Type 1 ENSO models (Figure 2c). These mean-state biases strongly alter ocean dynamical processes including equatorial upwelling and eastward shoaling of the thermocline, both of which are necessary for a proper Bjerknes feedback, and thus, these biases limit the skill of ENSO simulation in GCMs (e.g., Li & Hogan, 1999; Timmermann et al., 2007).

While denoting mean-state biases in Type 1 models in Figure 2, we refer to the difference from Type 2 models, but not from the observations. Given the clear differences in the mean-state and ENSO variability in the two types of models, we further explored the potential consequences of these biases for differences in the simulation of low-frequency variability. Type 1 ENSO models exhibit notable centennial-scale variability over the western Pacific (Figure 3c), which is absent in Type 2 models (Figure 3d). The highest amplitude centennial-scale SST variability (after 90 years low-pass filtering) in Type 1 ENSO models is colocated with the highest amplitude of high-frequency u10 fluctuations over the western equatorial Pacific (Figures 3a and 3c). In contrast, there is no such association in Type 2 ENSO models (Figures 3b and 3d). These results suggest that a westward extended cold tongue and ENSO variability bias may produce centennial-scale variability in the tropical Pacific.

We hypothesize that the centennial-scale SST variability in the western Pacific (Figures 3a and 3b) in Type 1 ENSO models results from the integration of the erroneously large u10 variability (Figures 3c and 3d), following the Hasselmann mechanism (Hasselmann, 1976). As the amplitude of u10 variability is significantly less over the western Pacific in Type 2 models, SST variability (Figure 3d) at the centennial timescale is relatively weak.

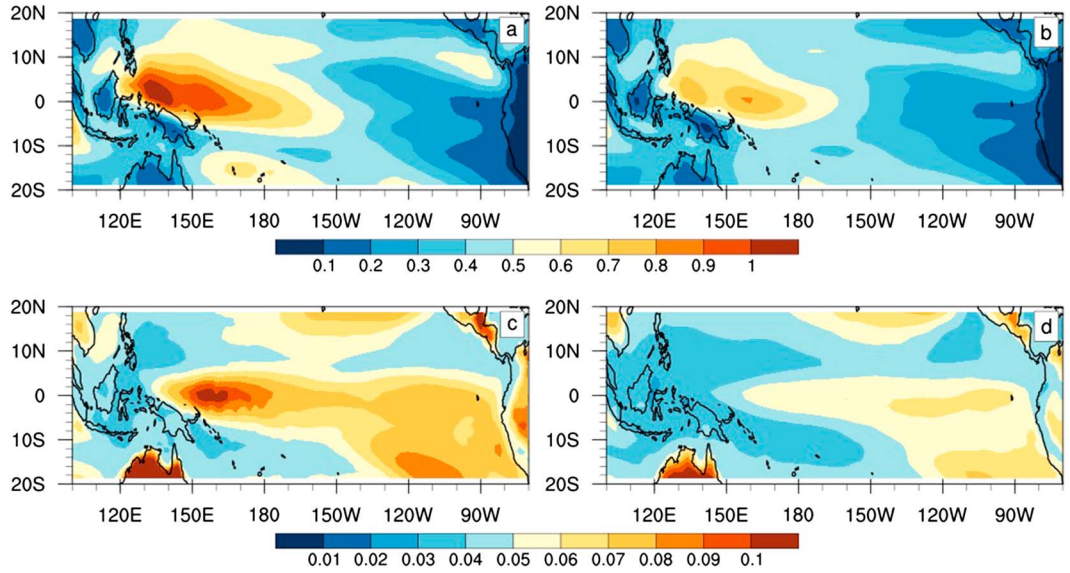

Figure 3. Association of high-frequency u10 with low-frequency SST. Composite standard deviation of (a, b) high-frequency (10-year high-pass filtered using Lanczos filter) u10 (m/s) and (c, d) low-frequency (90-year low-pass filtered using Lanczos filter) SST (°C). Type 1 ENSO models are shown in panels (a) and (c) and Type 2 ENSO models in panels (b) and (d). For reference, an observational estimate of (a) and (c) are given in Figure S7, albeit based on the relatively short instrumental record. u10= surface zonal wind speed; SST = sea surface temperature; ENSO = El Niño–Southern Oscillation.

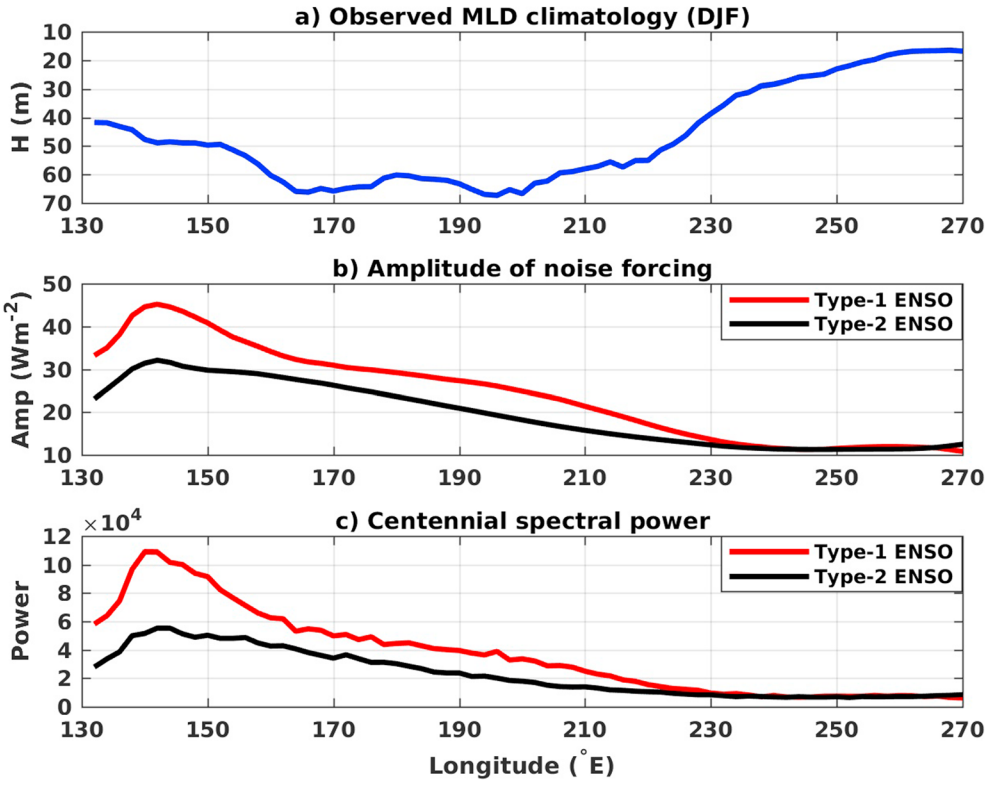

Figure 4. Prediction of centennial-scale variability using the Hasselmann model: (a) observed December-January-February (DJF) MLD (H) climatology (m), (b) amplitude of noise forcing (*A*) from u10 (W/m^2), and (c) centennial spectral power. The red and black curves in (b) and (c) indicate Type 1 and Type 2 ENSO models, respectively. The amplitude of noise forcing is multiplied by a scale factor of 25. The observed MLD climatology is based on 0.2 °C temperature difference data available from http://apdrc.soest.hawaii.edu/datadoc/mld.php. MLD = mixed layer depth; u10=surface zonal wind speed; ENSO = El Niño–Southern Oscillation.

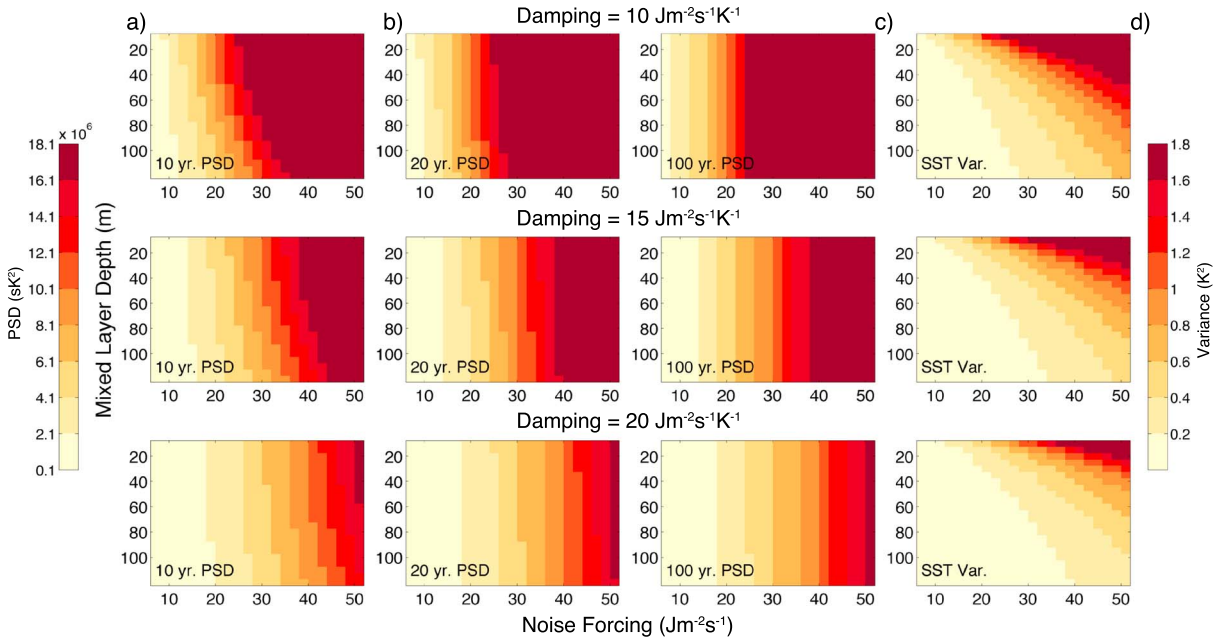

Figure 5. Power spectral density (PSD) from the analytical solution of the Hasselmann model for (a) 10-year, (b) 20-year, and (c) 100-year periods and (d) SST variance for different damping parameters. The horizontal axis shows the amplitude of noise forcing used in the Hasselmann model and the vertical axis the MLD. Greater noise amplitudes produce more power at all timescales and thus greater SST variance, but the deeper MLD decreases power except once it reaches longer timescales (i.e., centennial). Larger damping terms decrease both SST variance and centennial power. SST = sea surface temperature; MLD = mixed layer depth.

To examine our proposed hypothesis for the generation of centennial-scale variability in the western Pacific, we applied a stochastic model of climate variability following Hasselmann (1976). To do so, we calculated an exact analytical solution to the Hasselmann equation (see supporting information for the derivation). In the case of Type 1 ENSO models, the ENSO variability extends westward enough to penetrate the warm pool, implying injection of high-frequency, quasiperiodic and quasi-stochastic signals into the region. This results in significantly higher u10 variability over the western Pacific in Type 1 ENSO models and by consequence larger amplitude noise forcing to the Hasselmann model. Using longitudinal profiles of observed DJF climatology of MLD (H; Figure 4a), and zonal wind stress variability as the amplitude of noise forcing (*A*; Figure 4b), the models predict the structure and amplitude of the actual centennial variability of SST as a function of longitude. The results clearly show how the centennial power doubles in the western equatorial Pacific (Figure 4c), where the Type 1 models have a bullseye of centennial SST variability (Figure 3c), but the Type 2 ENSO models do not. In other words, the Hasselmann model does indeed predict the PCO given the amplitude of noise forcing. It is also noteworthy that the centennial-scale power (i.e., power spectral density or PSD) in the Hasselmann model output increases by ~100% in the western Pacific, despite the amplitude of the noise being prescribed in that area only increasing by ~38%. As observed climatological MLD (H) is prescribed for both types of models, the Hasselmann model demonstrates the impact of noise on centennial-scale variability. This result supports the hypothesis that centennial-scale variability in GCMs (i.e., as exhibited in Figure 3) emerges from high-frequency wind variability.

For additional confirmation of our proposed hypothesis for the generation of centennial-scale variability in the western Pacific, Figure 5 shows the PSD at 10-, 20-, and 100-year timescales for varying noise amplitudes, MLDs, and damping as well as the total SST variance that is produced. Intuitively, greater noise amplitudes produce greater PSD at all timescales and thus greater total SST variance. This SST variance is damped by deeper MLDs, which decrease power at all timescales. Importantly, however, the impact of MLD is smaller for longer timescales and has nearly no effect at the centennial timescales of interest, thus supporting the choice to use observed MLD for all models in the analysis in Figure 4. By varying a range of MLD and noise amplitude (which are the only things that can change in the Hasselmann model) in Figure 5, we also note that our set of experiments is functionally equivalent to one experiment wherein state-dependent noise forcing is introduced (Capotondi et al., 2018).

While the curves describing the Hasselmann predicted centennial PSD in Type 1 and Type 2 models in Figure 4b can be shifted up or down by changing the scaling of the noise forcing term (which is an estimate and thus uncertain in the construction of our model), their relative difference will stay largely the same. We cannot rule out the possibility that there are ocean dynamics or other physical processes contributing to the centennial-scale SST variability in GCMs such as that proposed by Karnauskas et al. (2012) related to the asymmetrical heat discharges during El Niño and La Niña events. The good agreement between the Hasselmann prediction and the actual GCM output (Figures 4b and 4c), however, is strong evidence that the simulated PCO arises solely from ocean integration of atmospheric noise. At a minimum, we cannot reject the null hypothesis that this variability is purely the reddening by the ocean of stochastic noise in the form of ENSO-related wind variability. This interpretation has critical implications for the PCO because the large amplitude noise in the western Pacific in Type 1 models results from relatively severe cold tongue extent and ENSO biases—by consequence, the PCO is also likely to be a GCM bias.

4. Summary and Discussion

Based on boreal wintertime SST variability in the western equatorial Pacific, we categorized 27 GCMs into two groups: Type 1 and Type 2 ENSO models. We found that mean-state biases in Type 1 ENSO models are related to an ENSO bias, which includes zonal wind variability in the western equatorial Pacific that is too strong relative to observations. Critically, this large wind variability produces spurious low-frequency variability via the Hasselmann mechanism—that is, the ocean integrates stochastic noise into low-frequency variability. The applications of the Hasselmann model also demonstrates that predictions of whether the PCO should exist in a real ocean or in other models can be determined based solely on their mean climatology and ENSO characteristics.

The mean-state of each GCM is different and differences in ENSO characteristics can reflect anything from random disturbances to modulation of ENSO itself from the background centennial-scale variability over the tropical Pacific (Fedorov & Philander, 2000). This leads to a familiar dilemma: Is the centennial variability a consequence of evolving ENSO characteristics or are the ENSO characteristics themselves driven by centennial variability? While the latter direction of causality may be important for some contexts, the underlying diversity (Capotondi et al., 2015) and complexity (Timmermann et al., 2018) of ENSO across models renders the processes by which centennial-scale variability modulate ENSO elusive.

Low-frequency climate variability can emerge internally through interactions within individual climate subcomponents or externally from variations in the solar insolation, volcanic eruptions, or changing atmospheric greenhouse gas concentrations (Latif, 1998; Latif & Keenlyside, 2011). A recent study (Ault et al., 2013) argued that centennial variability in CCSM4 originates as the thermodynamic response to external forcing; however, our results instead suggest that the origin lies, at least in part, in the interaction of internal variability with the mean-state as shown by Karnauskas et al. (2012). In fact, further analysis of historical simulations from Type 1 ENSO models (Figure S6) indicates a similar PCO pattern in historical runs, although the possibility of an additional response to anthropogenic forcing remains. The results presented herein not only suggest a mechanism for emergent centennial-scale variability (PCO) in the GCMs but also addresses the issues posed by an earlier study (Karnauskas et al., 2012) about the implications of the PCO. We found that the PCO is a spurious mode of variability arising due to biases in some GCMs. Despite being unrealistic in GCMs, the possibility that PCO may affect initialized hindcasts, as well as future projections, is a serious one. Therefore, it is important for climate forecasting and societal decision-making to account for this type of variability. In particular, caution should be exercised when interpreting results from Type 1 ENSO models, especially when predicting future climate by including these models in the multimodel ensemble. Whether a PCO exists in the real world or not may remain a mystery for some time due to the limited duration of instrumental records and the paucity of proxy records. Unless coupled models containing the ENSO bias featured in this study are fortuitously enabling a more realistic source of stochastic noise, our results suggest that if centennial-scale variability is indeed detected in records from the western Pacific, it is more likely to be a response to external forcing.

Acknowledgments

We are thankful to Prof. Richard Seager for useful discussions. This research was funded by Singapore Ministry of Education Academic Research Fund Tier 2 (Project MOE2016-T2-1-016). This work was also supported in part by the National Science Foundation under grants AGS-1243204, AGS-1401400, AGS-1602581, and OISE-1743738 and LDEO contribution 8258. We acknowledge the WCRP Working Group on Coupled Modeling and U.S. DOE/PCMDI for CMIP and thank the climate modeling groups (listed in the Table S1 of this paper) for producing and making available their model output (http://cmip-pcmdi.llnl.gov/cmip5/).

References

Arora, V. K., Scinocca, J. F., Boer, G. J., Christian, J. R., Denman, K. L., Flato, G. M., et al. (2011). Carbon emission limits required to satisfy future representative concentration pathways of greenhouse gases. *Geophysical Research Letters*, *38*, L05805. https://doi.org/10.1029/2010GL046270

Ault, T. R., Deser, C., Newman, M., & Emile-Geay, J. (2013). Characterizing decadal to centennial variability in the equatorial Pacific during the last millennium. *Geophysical Research Letters*, *40*, 3450–3456. https://doi.org/10.1002/grl.50647

Ault, T. R., St. George, S., Smerdon, J. E., Coats, S., Mankin, J. S., Carrillo, C. M., et al. (2018). A robust null hypothesis for the potential causes of megadrought in western North America. *Journal of Climate*, *31*(1), 3–24. https://doi.org/10.1175/JCLI-D-17-0154.1

Bentsen, M., Bethke, I., Debernard, J. B., Iversen, T., Kirkevåg, A., Seland, Ø., et al. (2013). The Norwegian earth system model, NorESM1-M—Part 1: Description and basic evaluation of the physical climate. *Geoscientific Model Development*, *6*(3), 687–720. https://doi.org/10.5194/gmd-6-687-2013

Bi, D., Dix, M., Marsland, S. J., O'Farrell, S., Rashid, H., Uotila, P., et al. (2013). The ACCESS coupled model: Description, control climate and evaluation. *Australian Meteorological and Oceanographic Journal*, *63*(1), 41–64. https://doi.org/10.22499/2.6301.004

Cai, W., Santoso, A., Wang, G., Yeh, S. W., An, S. I., Cobb, K. M., et al. (2015). ENSO and greenhouse warming. *Nature Climate Change*, *5*(9), 849–859. https://doi.org/10.1038/nclimate2743

Capotondi, A., Sardeshmukh, P. D., & Ricciardulli, L. (2018). The nature of the stochastic wind forcing of ENSO. *Journal of Climate*, *31*(19), 8081–8099. https://doi.org/10.1175/JCLI-D-17-0842.1

Capotondi, A., Wittenberg, A., & Masina, S. (2006). Spatial and temporal structure of tropical Pacific interannual variability in 20th century coupled simulations. *Ocean Modelling*, *15*(3–4), 274–298. https://doi.org/10.1016/j.ocemod.2006.02.004

Capotondi, A., Wittenberg, A. T., Newman, M., Di Lorenzo, E., Yu, J. Y., Braconnot, P., et al. (2015). Understanding ENSO diversity. *Bulletin of the American Meteorological Society*, *96*(6), 921–938. https://doi.org/10.1175/BAMS-D-13-00117.1

Clement, A., DiNezio, P., & Deser, C. (2011). Rethinking the Ocean's role in the southern oscillation. *Journal of Climate*, *24*(15), 4056–4072. https://doi.org/10.1175/2011JCLI3973.1

Clement, A. C., & Cane, M. (1999). A role for the tropical Pacific coupled ocean-atmosphere system on Milankovitch and millennial timescales. Part I: A modeling study of tropical Pacific variability. In *Mechanisms of Global Climate Change at Millennial Time Scales* (pp. 373–383). Washington, DC: American Geophysical Union. https://doi.org/10.1029/GM112p0363

Coats, S., & Karnauskas, K. B. (2017). Are simulated and observed twentieth century tropical Pacific Sea surface temperature trends significant relative to internal variability? *Geophysical Research Letters*, *44*, 9928–9937. https://doi.org/10.1002/2017GL074622

Coats, S., Smerdon, J. E., Cook, B. I., Seager, R., Cook, E. R., & Anchukaitis, K. J. (2016). Internal Ocean-atmosphere variability drives mega-droughts in Western North America. *Geophysical Research Letters*, *43*, 9886–9894. https://doi.org/10.1002/2016GL070105

Cobb, K. M., Charles, C. D., Cheng, H., & Edwards, R. L. (2003). El Niño/Southern Oscillation and tropical Pacific climate during the last millennium. *Nature*, *424*(6946), 271–276. https://doi.org/10.1038/nature01779

Collins, M., Tett, S., & Cooper, C. (2001). The internal climate variability of HadCM3 a version of the Hadley Centre coupled model without flux adjustments. *Climate Dynamics*, *17*(1), 61–81. https://doi.org/10.1007/s003820000094

Deser, C., Phillips, A. S., & Hurrell, J. W. (2004). Pacific Interdecadal climate variability: Linkages between the tropics and the North Pacific during boreal winter since 1900. *Journal of Climate*, *17*(16), 3109–3124. https://doi.org/10.1175/1520-0442(2004)017<3109:PICVLB>2.0.CO;2

Dommenget, D., & Latif, M. (2008). Generation of hyper climate modes. *Geophysical Research Letters*, *35*, L02706. https://doi.org/10.1029/2007GL031087

Donner, L. J., Wyman, B. L., Hemler, R. S., Horowitz, L. W., Ming, Y., Zhao, M., et al. (2011). The dynamical core, physical parameterizations, and basic simulation characteristics of the atmospheric component AM3 of the GFDL global coupled model CM3. *Journal of Climate*, *24*(13), 3484–3519. https://doi.org/10.1175/2011JCLI3955.1

Dufresne, J. L., Foujols, M. A., Denvil, S., Caubel, A., Marti, O., Aumont, O., et al. (2013). Climate change projections using the IPSL-CM5 Earth System Model: From CMIP3 to CMIP5. *Climate Dynamics*, *40*(9–10), 2123–2165. https://doi.org/10.1007/s00382-012-1636-1

Fedorov, A. V., & Philander, S. G. (2000). Is El Niño changing? *Science*, *288*(5473), 1997–2002. https://doi.org/10.1126/science.288.5473.1997

Gent, P. R., Danabasoglu, G., Donner, L. J., Holland, M. M., Hunke, E. C., Jayne, S. R., et al. (2011). The community climate system model version 4. *Journal of Climate*, *24*(19), 4973–4991. https://doi.org/10.1175/2011JCLI4083.1

Guilyardi, E. (2005). El Niño-mean-state seasonal cycle interactions in a multi-model ensemble. *Climate Dynamics*, *26*(4), 329–348. https://doi.org/10.1007/s00382-005-0084-6

Guilyardi, E., Wittenberg, A., Fedorov, A., Collins, M., Wang, C., Capotondi, A., et al. (2009). Understanding El Niño in ocean atmosphere general circulation models: Progress and challenges. *Bulletin of the American Meteorological Society*, *90*(3), 325–340. https://doi.org/10.1175/2008BAMS2387.1

Harrison, M. J., Rosati, A., Soden, B. J., Galanti, E., & Tziperman, E. (2002). An evaluation of AirSea flux products for ENSO simulation and prediction. *Monthly Weather Review*, *130*(3), 723–732. https://doi.org/10.1175/1520-0493(2002)130<0723:aeoasf>2.0.co;2

Hasselmann, K. (1976). Stochastic climate models part I. theory. *Tellus*, *28*(6), 473–485. https://doi.org/10.1111/j.2153-3490.1976.tb00696.x

Hua, W., Dai, A., & Qin, M. (2018). Contributions of internal variability and external forcing to the recent Pacific decadal variations. *Geophysical Research Letters*, *45*, 7084–7092. https://doi.org/10.1029/2018GL079033

Karnauskas, K. B., Murtugudde, R., & Busalacchi, A. J. (2007). The effect of the GaláPagos Islands on the equatorial Pacific cold tongue. *Journal of Physical Oceanography*, *37*(5), 1266–1281. https://doi.org/10.1175/jpo3048.1

Karnauskas, K. B., Seager, R., Kaplan, A., Kushnir, Y., & Cane, M. A. (2009). Observed strengthening of the Zonal Sea surface temperature gradient across the equatorial Pacific Ocean. *Journal of Climate*, *22*(16), 4316–4321. https://doi.org/10.1175/2009jcli2936.1

Karnauskas, K. B., Smerdon, J. E., Seager, R., & González-Rouco, J. F. (2012). A Pacific Centennial Oscillation predicted by coupled GCMs. *Journal of Climate*, *25*(17), 5943–5961. https://doi.org/10.1175/jcli-d-11-00421.1

Kay, J. E., Deser, C., Phillips, A., Mai, A., Hannay, C., Strand, G., et al. (2015). The Community Earth System Model (CESM) Large Ensemble Project: A community resource for studying climate change in the presence of internal climate variability. *Bulletin of the American Meteorological Society*, *96*(8), 1333–1349. https://doi.org/10.1175/bams-d-13-00255.1

Kim, S. T., Cai, W., Jin, F. F., & Yu, J. Y. (2014). ENSO stability in coupled climate models and its association with mean state. *Climate Dynamics*, *42*(11–12), 3313–3321. https://doi.org/10.1007/s00382-013-1833-6

Latif, M. (1998). Dynamics of Interdecadal variability in coupled ocean atmosphere models. *Journal of Climate*, *11*(4), 602–624. https://doi.org/10.1175/1520-0442(1998)011<0602:doivic>2.0.co;2

Latif, M., & Keenlyside, N. S. (2011). A perspective on decadal climate variability and predictability. *Deep Sea Research Part II: Topical Studies in Oceanography*, *58*(17–18), 1880–1894. https://doi.org/10.1016/j.dsr2.2010.10.066

Lemmon, D. E., & Karnauskas, K. B. (2018). A metric for quantifying El Niño pattern diversity with implications for ENSO–mean-state interaction. *Climate Dynamics*, 1–13. https://doi.org/10.1007/s00382-018-4194-3

Li, G., & Xie, S. P. (2014). Tropical biases in CMIP5 multimodel ensemble: The excessive equatorial Pacific cold tongue and double ITCZ problems. *Journal of Climate*, *27*(4), 1765–1780. https://doi.org/10.1175/JCLI-D-13-00337.1

Li, T., & Hogan, T. F. (1999). The role of the annual-mean climate on seasonal and interannual variability of the tropical Pacific in a coupled GCM. *Journal of Climate*, *12*(3), 780–792. https://doi.org/10.1175/1520-0442(1999)012<0780:trotam>2.0.co;2

Long, M. C., Lindsay, K., Peacock, S., Moore, J. K., & Doney, S. C. (2013). Twentieth-century oceanic carbon uptake and storage in CESM1 (BGC). *Journal of Climate*, *26*(18), 6775–6800. https://doi.org/10.1175/JCLI-D-12-00184.1

McPhaden, M. J., Lee, T., & McClurg, D. (2011). El Niño and its relationship to changing background conditions in the tropical Pacific Ocean. *Geophysical Research Letters*, *38*, L15709. https://doi.org/10.1029/2011GL048275

McPhaden, M. J., Zebiak, S. E., & Glantz, M. H. (2006). ENSO as an integrating concept in earth science. *Science*, *314*(5806), 1740–1745. https://doi.org/10.1126/science.1132588

Meehl, G. A., & Hu, A. (2006). Megadroughts in the Indian monsoon region and Southwest North America and a mechanism for associated multidecadal Pacific Sea surface temperature anomalies. *Journal of Climate*, *19*(9), 1605–1623. https://doi.org/10.1175/jcli3675.1

Newman, M., Shin, S., & Alexander, M. A. (2011). Natural variation in ENSO flavors. *Geophysical Research Letters*, *38*, L14705. https://doi.org/10.1029/2011gl047658

Philander, S. G. (2001). El Niño Southern Oscillation (ENSO) models. In *Encyclopedia of Ocean Sciences* (pp. 241–246). Academic Press. https://doi.org/10.1016/b978-012374473-9.00401-x

Philander, S. G., & Fedorov, A. (2003). Is El Niño sporadic or cyclic? *Annual Review of Earth and Planetary Sciences*, *31*(1), 579–594. https://doi.org/10.1146/annurev.earth.31.100901.141255

Raddatz, T. J., Reick, C. H., Knorr, W., Kattge, J., Roeckner, E., Schnur, R., et al. (2007). Will the tropical land biosphere dominate the climate–carbon cycle feedback during the twenty-first century? *Climate Dynamics*, *29*(6), 565–574. https://doi.org/10.1007/s00382-007-0247-8

Rotstayn, L. D., Jeffrey, S. J., Collier, M. A., Dravitzki, S. M., Hirst, A. C., Syktus, J. I., & et al. (2012). Aerosol-induced changes in summer rainfall and circulation in the Australasian region: A study using single-forcing climate simulations. *Atmospheric Chemistry and Physics Discussions*, *12*(2), 5107–5188. https://doi.org/10.5194/acpd-12-5107-2012

Schmidt, G. A., Ruedy, R., Hansen, J. E., Aleinov, I., Bell, N., Bauer, M., et al. (2006). Present-day atmospheric simulations using GISS ModelE: Comparison to in situ, satellite, and reanalysis data. *Journal of Climate*, *19*(2), 153–192. https://doi.org/10.1175/JCLI3612.1

Scoccimarro, E., Gualdi, S., Bellucci, A., Sanna, A., Giuseppe Fogli, P., Manzini, E., et al. (2011). Effects of tropical cyclones on ocean heat transport in a high-resolution coupled general circulation model. *Journal of Climate*, *24*(16), 4368–4384. https://doi.org/10.1175/2011JCLI4104.1

Seager, R., Tzanova, A., & Nakamura, J. (2009). Drought in the southeastern United States: Causes variability over the last millennium, and the potential for future hydroclimate change. *Journal of Climate*, *22*(19), 5021–5045. https://doi.org/10.1175/2009jcli2683.1

Seager, R., & Vecchi, G. A. (2010). Greenhouse warming and the 21st century hydroclimate of southwestern North America. *Proceedings of the National Academy of Sciences of the United States of America*, *107*(50), 21,277–21,282. https://doi.org/10.1073/pnas.0910856107

Sun, D.-Z., & Liu, Z. (1996). Dynamic Ocean-atmosphere coupling: A thermostat for the tropics. *Science*, *272*(5265), 1148–1150. https://doi.org/10.1126/science.272.5265.1148

Taylor, K. E., Stouffer, R. J., & Meehl, G. A. (2012). An overview of CMIP5 and the experiment design. *Bulletin of the American Meteorological Society*, *93*(4), 485–498. https://doi.org/10.1175/bams-d-11-00094.1

Tierney, J. E., Oppo, D. W., Rosenthal, Y., Russell, J. M., & Linsley, B. K. (2010). Coordinated hydrological regimes in the indo-Pacific region during the past two millennia. *Paleoceanography*, *25*, PA1102. https://doi.org/10.1029/2009pa001871

Timmermann, A., An, S. I., Kug, J. S., Jin, F. F., Cai, W., Capotondi, A., et al. (2018). El Nino–Southern Oscillation complexity. *Nature*, *559*(7715), 535–545. https://doi.org/10.1038/s41586-018-0252-6

Timmermann, A., Okumura, Y., An, S.-I., Clement, A., Dong, B., Guilyardi, E., et al. (2007). The influence of a weakening of the Atlantic Meridional overturning circulation on ENSO. *Journal of Climate*, *20*(19), 4899–4919. https://doi.org/10.1175/jcli4283.1

Trenberth, K. E., & Hurrell, J. W. (1994). Decadal Atmosphere-Ocean variations in the Pacific. *Climate Dynamics*, *9*(6), 303–319. https://doi.org/10.1007/bf00204745

van Oldenborgh, G. J., Philip, S. Y., & Collins, M. (2005). El Niño in a changing climate: A multi-model study. *Ocean Science*, *1*(2), 81–95. https://doi.org/10.5194/os-1-81-2005

Volodin, E. M., Dianskii, N. A., & Gusev, A. V. (2010). Simulating present-day climate with the INMCM4. 0 coupled model of the atmospheric and oceanic general circulations. *Izvestiya, Atmospheric and Oceanic Physics*, *46*(4), 414–431. https://doi.org/10.1134/S000143381004002X

Watanabe, S., Hajima, T., Sudo, K., Nagashima, T., Takemura, T., Okajima, H., et al. (2011). MIROC-ESM 2010: Model description and basic results of CMIP5-20c3m experiments. *Geoscientific Model Development*, *4*(4), 845–872. https://doi.org/10.5194/gmd-4-845-2011

Wittenberg, A. T. (2009). Are historical records sufficient to constrain ENSO simulations? *Geophysical Research Letters*, *36*, L12702. https://doi.org/10.1029/2009gl038710

Xie, S. P., Miyama, T., Wang, Y., Xu, H., De Szoeke, S. P., Small, R. J. O., et al. (2007). A regional ocean–atmosphere model for eastern Pacific climate: Toward reducing tropical biases. *Journal of Climate*, *20*(8), 1504–1522. https://doi.org/10.1175/JCLI4080.1

Xin, X.-G., Wu, T.-W., Li, J.-L., Wang, Z.-Z., Li, W.-P., & Wu, F.-H. (2013). How well does BCC_CSM1. 1 reproduce the 20th century climate change over China? *Atmospheric and Oceanic Science Letters*, *6*(1), 21–26.

Yongqiang, Y., Xuehong, Z., & Yufu, G. (2004). Global coupled ocean-atmosphere general circulation models in LASG/IAP. *Advances in Atmospheric Sciences*, *21*(3), 444–455. https://doi.org/10.1007/BF02915571

Zebiak, S. E., & Cane, M. A. (1991). Natural climate variability in a coupled model. In *Greenhouse-gas-induced climatic change: A critical appraisal of simulations and observations* (pp. 457–469). Elsevier. https://doi.org/10.1016/b978-0-444-88351-3.50036-2